Chapter 1

Geometric, Stochastic and Algebraic Vortices

Nicholas Kevlahan
Department of Mathematics & Statistics
McMaster University, Hamilton, Ontario, Canada

Dedicated to Lu Ting on his eightieth birthday

Abstract

Mathematical concepts can often be understood in one of three complementary ways: geometric, algebraic or stochastic. In this chapter I show how vortices may be interpreted in each of these three ways. Each point of view is appropriate for certain applications, and each sheds new light on the role played by vortices in fluid dynamics. This review is necessarily brief, and makes no attempt to be exhaustive, but I hope it gives an interesting overview of vortices in all their forms.

1.1 Introduction

Before examining the different ways of representing the vortices, it is natural say a few words about why vortices are interesting and important to study. A vortex may be defined as a region of flow characterized by significant coherent vorticity $\boldsymbol{\omega}$, where vorticity is the curl of velocity,

$$\boldsymbol{\omega} = \nabla \times \boldsymbol{u}. \tag{1.1}$$

Coherence here means both coherence in space (e.g. a connected identifiable shape, usually tube-like), and coherence in time (e.g. the shape

can be followed for a significant length of time). This definition is deliberately vague: the precise meaning of the word vortex in fluid dynamics has been the subject of long and intense debate (see for example [4; 16] for a comparison of different definitions). Even the vague definition stated above is not unbiased; it has a definite geometric or topological flavour. A purely stochastic or statistical definition is also possible. Farge, Schneider & Kevlahan [10] proposed to define the vortices of two-dimensional turbulence as the non-Gaussian part of the vorticity field, i.e. that part which is left over when the vorticity is de-noised. Moreover, an algebraic understanding of vortices is used in numerical vortex methods. In vortex methods the solution of the vorticity equation (a partial differential equation) is reduced to a set of algebraic equations for the positions and strengths of vortex elements [7]. These vortex elements have very little geometry: in most cases they are nothing more than points. Even the definition of the word vortex depends on whether we take a geometric, stochastic or algebraic point of view.

Why have people put so much effort into defining and understanding vortices? First, we are drawn to vortices because they are beautiful and ubiquitous features of fluid flows. People have been fascinated by their persistence (e.g. leap-frogging smoke rings) and by their structure (e.g. the von Karman vortex street behind a bluff body). In turbulent flows the vortices are the only obvious organized structures in a sea of random fluctuations. Vorticity is also attractive mathematically since the vorticity equation is simpler than the primitive form of the Navier–Stokes equations, especially in two dimensions. For example, in two-dimensional inviscid flows all functionals of vorticity are conserved, and in three-dimensional inviscid flows the integral of helicity is conserved (which means the linking number of vortex rings is invariant). Unfortunately, the vorticity field is actually quite difficult to measure experimentally.

Vortices are also important because they control the dynamics of many useful flows. An indication of the prominence of vortices in fluid dynamics is given by the fact that the word 'vortex' or 'vortices' occurs in the titles of ten articles in the *Annual Review of Fluid Dynamics* in the last ten years (an average of one article on vortices per issue). Perhaps the best-known example is the starting vortex around an airfoil (which generates lift as a consequence of Kelvin's circulation theorem). Other examples include the use of vortices to improving mixing, the transport of pollutants in the atmosphere and oceans by vortices [35], and the generation of vorticity (and hence turbulence) by curved shocks [20]. We now consider two important

vortex-dominated flows in more detail.

A good example of the key role of vortices is fluid–structure interaction at moderate Reynolds numbers (say $100 < \mathrm{Re} < 300$). Well-defined coherent vortices are generated via the no-slip boundary condition at the surface of a bluff body. These vortices exert a force on the body which causes it to move or vibrate. The aeolian noise generate by the wind blowing through telephone wires is the most familiar example of this. Swimming fish use controlled vortex-induced vibration to swim. More dramatic examples include the destruction of buildings (e.g. the Tacoma narrows bridge in 1940 and the Ferrybridge nuclear station cooling towers in 1965) and machines (e.g. heat exchanger tube bundles can shake themselves apart). Vortex-induced vibration is a major area of engineering research, and controlling it is vital for the construction of bridges, large buildings, airplanes and off-shore drilling platforms.

The precise role of vortices in fluid–structure interaction was recently clarified in a paper by Noca et al. [32; 33]. They showed that the force on a body exerted by an vortical flow is given by

$$\begin{aligned}\boldsymbol{F}(t) = &-\frac{1}{\mathcal{N}-1}\frac{d}{dt}\int_{V_\infty} \boldsymbol{x}\times\boldsymbol{\omega}\,\mathrm{d}V \\ &-\frac{1}{\mathcal{N}-1}\frac{d}{dt}\oint_{S_b(t)} \boldsymbol{x}\times(\boldsymbol{n}\times\boldsymbol{u})\,\mathrm{d}S - \oint_{S_b(t)} \boldsymbol{n}\cdot(\boldsymbol{u}-\boldsymbol{u}_S)\,\mathrm{d}S, \end{aligned} \tag{1.2}$$

where $\boldsymbol{n}$ is the inward-pointing normal vector of the body surface, $\mathcal{N}$ is the dimension of the space, V_∞ is the (infinite) fluid volume, $S_b(t)$ is the body surface and $\boldsymbol{u}_S$ is the velocity of the surface. If we assume a no-slip boundary condition at the surface of the body, and that the body is stationary and non-rotating, then

$$\boldsymbol{F}(t) = -\frac{1}{\mathcal{N}-1}\frac{d}{dt}\int_{V_\infty} \boldsymbol{x}\times\boldsymbol{\omega}\,\mathrm{d}V. \tag{1.3}$$

Note that (1.3) says that the force on the body is equal and opposite to the change in the fluid impulse. Equation (1.3) shows very clearly that the fluid forces on a body are due entirely to the movement and changing shape of the vortices.

Sound or noise is another phenomenon which may be related directly to vortex structure and dynamics. Kambe et al. [18] (following Lighthill [28]) showed that vortices generate a far-field sound wave with pressure given by

$$p_F = -\frac{\varepsilon^{(1)}(t_r)}{15\pi c^2 r} - \frac{\rho_0}{c^2}Q^{(3)}_{ij}(t_r)\frac{x_i x_j}{r^3} + \frac{\rho_0}{c^3}Q^{(4)}_{ijk}(t_r)\frac{x_i x_j x_k}{r^4} + \cdots \tag{1.4}$$

where the superscript (n) indicates the n-th time derivative, $t_r = t - r/c$ is the retarded time, $\varepsilon(t)$ is rate of dissipation of energy, c is the speed of sound, $r = |\boldsymbol{x}|$ is the distance from the vortex source, and

$$Q_{ij}(t) = -\frac{1}{12\pi}\int (\boldsymbol{y}\times\boldsymbol{\omega})_i\, y_j \,\mathrm{d}^3\boldsymbol{y},$$
$$Q_{ijk}(t) = \frac{1}{32\pi}\int (\boldsymbol{y}\times\boldsymbol{\omega})_i\, y_j y_k \,\mathrm{d}^3\boldsymbol{y},$$

are moments of the vorticity distribution. Equation (1.4) clearly shows how changes in the configuration or shape of vortices directly generates sound. In the same paper Kambe et al. present results from experiments which show how colliding vortex rings create a sound burst. This is a nice example of how changes in vortex topology can have a practically important effect. Reducing aircraft noise may depend on a better understanding of how vortices interact!

As mentioned earlier, vortices are also considered to be key to understanding turbulence. The principal obstacle in dealing with turbulence, both numerically and analytically, is the fact that high Reynolds number turbulence contains a huge range of active length and time scales. A naive estimate (which ignores intermittency) suggests that the number of space–time degrees of freedom in a turbulent flow increases like Re^3. In atmospheric turbulence the active length scales range from millimetres to tens or hundreds of kilometres! This range of scales is also continuous, which means the usual separation of scales techniques (e.g. WKB) are not applicable. A different way of reducing the dimensionality of the problem must be found. The fact that turbulence contains coherent vortices, and that vortices may control much of the dynamics of the flow, has suggested a new way of tackling the problem [10]. One can divide turbulence into the coherent vortices (which are calculated exactly), and the rest of the flow (defined to be noise, whose effect can be modelled statistically). In this approach the problem of turbulence is reduced to vortex dynamics. Because turbulence is intermittent, the coherent vortices are conjectured to take up an increasingly small part of the flow as the Reynolds number increase, resulting in a significant reduction in the dimensionality of the problem. The simplest example of this approach is large eddy simulation (LES) where the coherent vortices are taken to be the largest Fourier modes of the flow [27]. More sophisticated methods using adaptive wavelet filtering to include all scales of the coherent vortices are also being attempted [13; 14; 19; 38].

The transition to turbulence is also characterized by changes in vortex structure and dynamics. One of the clearest examples is the flow past a cylinder as Reynolds number increases. Frisch [11] shows a beautiful sequence of visualizations of the vorticity as a function of Reynolds number. He comments that the spatial and temporal symmetries of the vorticity field are progressively lost as Reynolds number gradually increases, only to be recovered statistically in fully developed turbulence at high Reynolds number. In this case, as for all bounded flows, much of the turbulence originates in the wall vortices of the boundary layer. An understanding of vorticity production in the boundary layer is also thought to be essential for calculating the mean velocity profile of in channel or pipe flow [31].

We have seen that vortices dominate useful flows, as well as being attractive mathematically and visually beautiful in their own right. The rest of this paper sketches how vortices may be represented in three complementary ways: geometric, stochastic and algebraic. The geometric (or topological) point of view is described in section 1.2, with a particular emphasis on the coherent vortices of turbulence. Section 1.3 considers two versions of the stochastic approach: a probabilistic representation of the vorticity equation, and a wavelet de-noising definition of coherent vortices. The algebraic vortex is represented in section 1.4 by two numerical schemes: the vortex method, and the adaptive wavelet collocation method for the vorticity equation. Finally, we make some concluding comments in section 1.5.

1.2 Geometric vortices

1.2.1 *Conservation laws*

The most obvious way of characterizing vortices is based on their geometry and topology. Geometric vortices are defined in terms of their shape, and how this shape changes in time through interaction with other vortices or self advection. Let us recall the three-dimensional incompressible vorticity equation,

$$D_t\boldsymbol{\omega} = (\boldsymbol{\omega}\cdot\nabla)\boldsymbol{u} + \nu\Delta\boldsymbol{\omega}, \tag{1.5}$$

where the D_t is the material derivative, and the velocity $\boldsymbol{u}$ is related to the vorticity via the Biot–Savart law (which makes the equation nonlinear). The first term on the right hand side of (1.5) is the change in vorticity due to vortex stretching (which is identically zero in two dimensions), and the second term is the diffusion of vorticity (which spreads vorticity out,

and is essential for vortex reconnection). The geometrical and topological constraints on this equation are much simpler (and exact) if we set $\nu = 0$, which gives the inviscid equations. In this case one can prove a number of interesting conservation laws [30].

The best known conservation law is Kelvin's circulation theorem

$$D_t \left(\int_{S(t)} \boldsymbol{\omega} \cdot \mathrm{d}\boldsymbol{S} \right) = 0 \tag{1.6}$$

which states that the vorticity flux through a material surface $S(t)$ is conserved. Helicity is also conserved

$$D_t \left(\int_{\mathbb{R}^3} \boldsymbol{u} \cdot \boldsymbol{\omega} \, \mathrm{d}\boldsymbol{x} \right) = 0, \tag{1.7}$$

which means that the linking number of vortex rings is conserved (they cannot be unlinked). The fluid impulse and the moment of the fluid impulse are also conserved. In two dimensions, because the vortex stretching term is absent, all functionals of vorticity are conserved (including all L^p norms).

1.2.2 *Slender vortices*

The simplest geometrical vortices are vortex lines (i.e. the circulation is concentrated on a curve in $\mathbb{R}^3$). These curves move with the fluid, and must end at solid boundaries or form loops. Although a vortex line is an elegant and natural idealization of a vortex, it has the disadvantage that any non-zero curvature causes it to move infinitely fast! The concept of a *slender* vortex has therefore been developed to correct this problem [21; 22; 30; 37]. The simplest version of the slender vortex approximation [40] is the self-induction equation for an isolated filament

$$\frac{\partial \boldsymbol{X}}{\partial t} = \kappa \boldsymbol{b}, \tag{1.8}$$

where $\boldsymbol{X}(s,t)$ is the centreline of the vortex, $\kappa(s,t)$ is its curvature and $\boldsymbol{b}(s,t)$ is the binormal to the curve. Note that in the self-induction approximation the thickness δ of the vortex filament does not appear explicitly (although it has been absorbed into the time via the re-scaling $t = \log(1/\delta)\, t'$). The effect of other filaments may be included via the Biot–Savart law, provided the separation between filaments remains much greater than δ.

Slender vortex models have the advantage that the conservation laws of inviscid flow stated above are remain valid. The disadvantage is that

slender vortex models are only valid as long as the vortices remain well-separated. This means they cannot treat vortex reconnection or topology change. In addition, Zhou [44] has shown that these models can produce unphysical results because the core width is uniform along the vortex and does not change in time. Despite these shortcomings, the simplicity of slender vortices make them attractive mathematically. They have been used to examine the early stages of vortex interaction [23], and to understand some aspects of turbulence [37]. Interestingly, slender vortex models appear to be almost exact when applied to the quantized vortices of superfluids.

1.2.3 *Diffusive vortices*

Less mathematical, but more practically useful, geometric definitions of vortices have been developed to extract (or *educe*) vortices from experimental and numerical data. Bonnet et al. [4] made a comprehensive comparison of the most popular techniques. Because real vortices are diffusive, their definition must also be a bit fuzzy. The simplest approach is to threshold on the L^1 or L^2 norm of vorticity. Figure 1.1 shows isosurfaces of vorticity from the $4\,096^2$ direct numerical simulation (DNS) of Yokokawa *etal.* [43]. The isosurfaces reveal that the vortices are tube-like and fill much of the turbulence (although they are not distributed completely homogeneously). The effect of these vortices on flow dynamics and kinematics can be evaluated by conditional averaging on the thresholded vorticity. More sophisticated approaches attempt to include the temporal, as well as spatial, coherence of the vorticity.

The goal of vortex eduction is to determine if characteristics of the flow as a whole can be explained by the vortices alone. Such an approach has been quite successful when the flow includes large coherent vortices with relatively simply dynamics (such as in mixing layers, jets, and in the fluid–structure interaction at moderate Reynolds numbers). Vortex eduction has also been used extensively to investigate near-wall turbulence (which led to the discovery of hair-pin vortices), and the transition to turbulence on a flat plate. Another major application of vortex eduction has been the attempt to determine whether turbulence is contains coherent vortices and, if so, whether these vortices control the dynamics of the flow. It is now clear that the answer to the first question if yes: all turbulent flows are full of coherent vortices which are tube-like and persist for a significant time [17]. The answer to the second question is not so clear: vortices appear to be an essential part of turbulence, but they may not always control its dynamics.

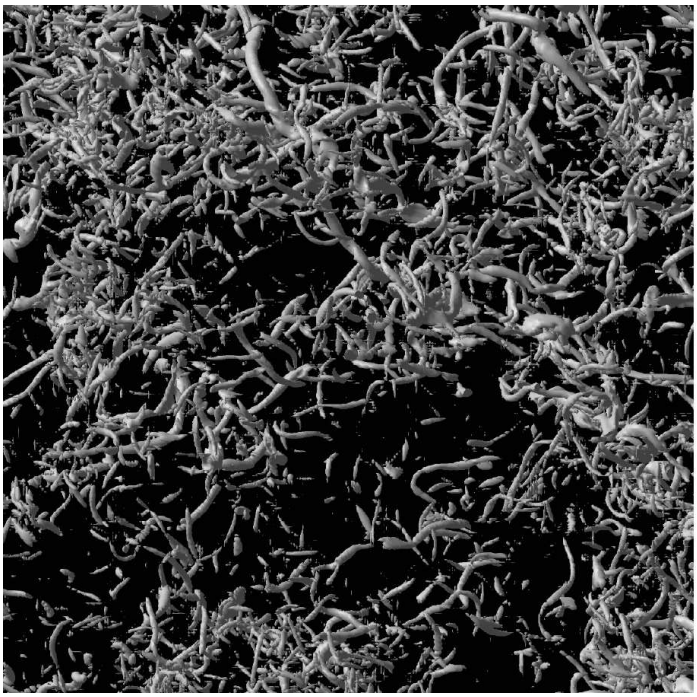

Fig. 1.1 Yokokawa eta al.'s [42] DNS of homogeneous isotropic turbulence at $\mathrm{Re}_\lambda = 1\,217$. The figure shows isosurfaces of vorticity of at the level $\bar{\boldsymbol{\omega}} + 4\sigma$, where $\bar{\boldsymbol{\omega}}$ is the mean vorticity and σ is its standard deviation. The region shown is $(748^2 \times 1\,496)\eta$, where η is the Kolmogorov length.

The geometric approach includes the mathematically attractive slender vortex model, and many types of vortex eduction for real flows. However, shape and topology are not always the most useful ways of representing vortices. In the following section we will see how a stochastic point of view can provide insight not available from geometry alone. We will also see how the vorticity equations themselves may be cast in an entirely probabilistic form.

1.3 Stochastic vortices

1.3.1 *Proper orthogonal decomposition*

Perhaps the oldest stochastic (or statistical) representation of vortices is the proper orthogonal decomposition (POD). The POD was introduced

by Lumley [29], and has since become one of the standard tools for analyzing vortical flows [3]. POD (which is also known Karhunen–Loève decomposition, or principal components analysis) decomposes a turbulent velocity field into an ordered set of orthogonal eigenfunctions $\phi^{(n)}(\boldsymbol{x})$ $(n = 1, 2, 3, \ldots, N)$, which are solutions of the linear eigenvalue problem

$$\int R_{ij}(\boldsymbol{x}, \boldsymbol{x}')\, \phi_j^{(n)}(\boldsymbol{x}')\, \mathrm{d}\boldsymbol{x}' = \lambda^{(n)} \phi_i^{(n)}(\boldsymbol{x}),$$

where $R_{ij}(\boldsymbol{x}, \boldsymbol{x}') = \langle \boldsymbol{u}(\boldsymbol{x}) \boldsymbol{u}^*(\boldsymbol{x}') \rangle$ is the two-point correlation tensor. The first N eigenfunctions provide an optimal N-term representation of the flow in terms of the L^2, or energy, norm. In addition, if the eigenvalues $\lambda^{(n)}$ decrease rapidly with n, and the flow is periodic or statistically stationary in time, the first eigenmode is a good representation of a typical coherent vortex. This is true for most mixing layers and jets. POD may also be interpreted as a generalized Fourier transform since, if the flow is homogeneous in space, the eigenfunctions are Fourier modes (the 'eddies' of classical homogeneous isotropic turbulence).

POD can be used to construct a reduced model of a turbulent flow by retaining only the first few eigenfunctions. This model captures the most important structure of the flow (as measured by energy), and may be used to clarify its dynamics. One must be careful, however, in interpreting POD eigenfunctions as geometric vortices. In fact, the POD eigenfunctions are only statistically representative of the average kinetic energy of the flow: there is no guarantee that they resemble the vortices in any particular flow realization. This is especially obvious in the case of homogeneous turbulence, where the most energetic Fourier mode (at the integral scale) does not resemble a real vortex! Indeed, most kinetic energy is at the integral scale $O(1)$, while most enstrophy is at the much smaller Taylor scale $O(\mathrm{Re}^{-1/2})$. POD vortices are therefore not (in general) the same as the geometric vortices of the previous section. Bonnet et al. [4] compares the POD statistical vortices with other, more geometric, eduction techniques.

1.3.2 *A de-noising definition of coherent vortices*

Instead of trying to find the optimal N-term representation for the kinetic energy of a flow, one can define vortices statistically in terms of their coherence. Farge et al. [10] have proposed defining the vortices of turbulence as that part of the flow which is not Gaussian noise. The basic idea is to use nonlinear wavelet filtering of the vorticity field to remove additive Gaussian

noise from the vorticity. The wavelet modes associated with the noise are discarded, and the vortices are reconstructed from the remaining wavelet modes.

This approach is based on Donoho's [9] optimal de-noising theorem for additive Gaussian white noise. The theorem states that the optimal way to de-noise a signal ω sampled on N points and perturbed by an additive Gaussian white noise of variance σ is to take its orthonormal wavelet transform, and then retain only those wavelet coefficients with absolute value larger than the threshold $\epsilon_D = (2\sigma \log N)^{1/2}$ before reconstructing the de-noised signal $\omega_>$. In the case of turbulence, $\omega_>$ is then *defined* to be the coherent vortices of the flow.

Unfortunately, Donoho's theorem cannot be applied directly to a turbulent vorticity field. First, because we do not know in advance that the noise is Gaussian, and secondly because we do not know its variance. Moreover, the statistical theory of homogeneous turbulence suggests that the noise may be coloured rather than white (i.e. the noise may depend on the length scale). In order to address these difficulties Farge et al. proposed an iterative de-noising algorithm. In the first iteration the variance of the noise is taken to be equal to the variance of the vorticity field, and the noise is extracted. Because this is an overestimation, some coherence will remain in the noise, and so the filtering is repeated on the noise alone. The coherent part of the noise is then combined with the coherent vorticity extracted in the first iteration. This procedure is repeated until the noise is Gaussian to within the desired tolerance. In practice, for two-dimensional turbulence one iteration is often sufficient.

Farge et al. applied this algorithm to extract the coherent vortices from a 256^2 DNS of two-dimensional turbulence and found that the coherent vortices represent just 0.7% of the wavelet modes, but contain 94% of the enstrophy. Furthermore, the coherent vortices closely resemble the vortices defined using geometrical techniques, such the Q-criterion [15; 16].

By applying this wavelet de-noising at each time step, and modelling the effect of the neglected modes statistically, one obtains coherent vortex simulation (CVS). CVS assumes that the coherent vortices (defined in the specific way described here) control the dynamics of the flow. If some noise is retained along with the coherent vortices, one obtains wavelet direct numerical simulation (WNDS), where the effect of the neglected modes is not included. WDNS will be described in detail in section 1.4.

In both POD and CVS the vortices are defined statistically, but this definition is still based on the usual deterministic vorticity equation (1.5). We

now consider a probabilistic representation of the vorticity equation itself, where the vortices (defined as particles) are reduced to random variables.

1.3.3 *A probabilistic version of the vorticity equation*

As mentioned in the introduction, most mathematical concepts may be expressed in either geometrical, stochastic or algebraic form. In particular, many partial differential equations (PDEs) can be associated to a stochastic differential equation (SDE). Or rather, a Langevin type SDE has an associated PDE (called the Fokker–Planck equation) which describes the time evolution of the probability density function (PDF) of its solution (which is a random variable).

For example, one can associate to the three-dimensional linear advection–diffusion equation

$$\frac{\partial \boldsymbol{f}}{\partial t} = \boldsymbol{v} \cdot \nabla \boldsymbol{f} + \nu \Delta \boldsymbol{f} \tag{1.9}$$

an SDE for the stochastic process $\boldsymbol{X}(t; \boldsymbol{X}_0) \in \mathbb{R}^3$

$$d\boldsymbol{X}(t) = \boldsymbol{v}(t, \boldsymbol{X}(t)) + \sqrt{2\nu}\, \mathrm{d}\boldsymbol{W}_t, \tag{1.10}$$

where $\boldsymbol{W}_t$ is a three-dimensional Brownian motion. The PDF of the random variable $\boldsymbol{X}(t)$ is the solution $\boldsymbol{f}(t)$ of the advection–diffusion equation.

Comparing equation (1.9) to the two-dimensional vorticity equation

$$\frac{\partial \boldsymbol{\omega}}{\partial t} = \boldsymbol{u} \cdot \nabla \boldsymbol{\omega} + \nu \Delta \boldsymbol{\omega} \tag{1.11}$$

suggests that we should be able to find its associated Langevin equation (where $\boldsymbol{X}(t)$ becomes the Lagrangian trajectory of a stochastic point vortex). The problem is that in equation (1.11) the advecting velocity is not known in advance; it depends on the vorticity $\boldsymbol{\omega} = \nabla \times \boldsymbol{u}$. This means we require an additional SDE for the velocity, and we need to solve a coupled system of nonlinear SDEs.

In a recent paper Busnello et al. [5] derived just such an SDE for the three-dimensional vorticity equation. The vorticity and velocity are given by

$$\boldsymbol{\omega}(\boldsymbol{x}, t) = \boldsymbol{E}[U_t^{x,t} \boldsymbol{\omega}_0(X_t^{x,t})], \tag{1.12}$$

$$\boldsymbol{u}(\boldsymbol{x}, t) = \frac{1}{2} \int_0^\infty \frac{1}{s} \boldsymbol{E}[\boldsymbol{\omega}(\boldsymbol{x} + \boldsymbol{W}_s, t) \times \boldsymbol{W}_s]\, \mathrm{d}s, \tag{1.13}$$

where $\boldsymbol{E}[\cdot]$ is the expectation. Equation (1.13) is the stochastic form of the Biot–Savart law. The vorticity is thus a weighted average over the Lagrangian paths $(\boldsymbol{X}_s^{x,t})_{0\leq s\leq t}$ of the stochastic point vortices, which are solutions of the following SDEs

$$\begin{aligned} \mathrm{d}\boldsymbol{X}_s^{x,t} &= -\boldsymbol{u}(X_s^{s,t}, t-s)\,\mathrm{d}s + \sqrt{2\nu}\,\mathrm{d}\boldsymbol{W}_s, \quad s \leq t, \\ X_0^{x,t} &= x. \end{aligned} \tag{1.14}$$

The deformation matrices $(U_s^{x,t})_{0\leq s\leq t}$ are themselves solutions to the following SDEs with random coefficients

$$\begin{aligned} \mathrm{d}U_s^{x,t} &= U_s^{x,t}\mathcal{D}_u(X_s^{x,t}, t-s)\,\mathrm{d}s, \quad s \leq t, \\ U_0^{x,t} &= I, \end{aligned} \tag{1.15}$$

where $\mathcal{D}_u = 1/2(\nabla\boldsymbol{u} + \nabla\boldsymbol{u}^T)$ is the deformation tensor.

Although the probabilistic representation given above is rather complicated, and is unlikely to simplify the solution of the vorticity equation, it is nevertheless interesting. First, because it proves that there is a rigorous and exact SDE representation of the vorticity equation, in line with our intuition. Secondly, because it shows that the continuous vorticity equation has an exact representation in terms of Lagrangian point vortices. Finally, the SDE is the analytical version of the numerical vortex methods which are discussed in the following section. Thus, this SDE may help us develop alternative numerical vortex methods. It is also possible that a careful analysis of the SDE form of the vorticity equation will suggest new analytical approximations which are not obvious from the usual PDE form.

1.4 Algebraic vortices

1.4.1 *Numerical vortex methods*

We now consider the third and final class of vortices: algebraic vortices. By algebraic vortices we mean vortices used as computational elements to reduce the vorticity PDE to a system of algebraic equations. This algebraic system is then solved using the techniques of numerical linear algebra. Algebraic vortices are therefore a sort of basis for the vorticity equation. The vortices themselves generally have no internal degrees of freedom.

In a sense, the most primitive numerical vortex method is pseudo-spectral simulation. In this method the vortices are the *eddies* of the homogeneous isotropic turbulence, i.e. Fourier modes of different wave-

lengths. Indeed, in large eddy simulation (LES) this connection is explicit: the flow is represented by the largest (and hence most energetic) eddies.

Usually, however, the term *vortex method* is reserved for those methods that discretize the vorticity equation using computational elements in physical space, and use a Lagrangian or semi-Lagrangian version of the vorticity equations. Vortex methods date back to Prager [34] and Rosenhead [36] in the 1920s and 1930s, but were not commonly used (or justified mathematically) until the work of Chorin [6], Majda [1; 2] Leonard [26], Krasny [25] and others. Although vortex methods are usually applied to two-dimensional flows, a highly accurate three-dimensional vortex method for wake flows was developed recently by Cottet & Poncet [8]. In this section we sketch the basics of two-dimensional vortex methods, and relate these algebraic vortices to the geometric and stochastic vortices described earlier. Cottet & Koumoutsakos [7] have published a very nice overview of the subject, which the reader should consult for more details on vortex methods.

Two-dimensional vortex methods first sample the circulation of the initial vorticity field onto a finite number N of points (i.e. vortex particles). The vorticity equations are then integrated in time from this initial condition using a two-step method:

(1) **Inviscid step.** The particles are moved by Lagrangian advection due to the velocity field of all other particles (according to Kelvin's circulation theorem 1.6, the circulation of the particles is unchanged).
(2) **Viscous step.** Vorticity diffusion is modelled by exchanging circulation amongst nearby particles (particle strength exchange), or by perturbing the particle's position by white noise to model Brownian diffusion (this is much less accurate).

Since these two steps do not commute, the time accuracy of the method is limited to second-order.

To obtain a stable numerical method, one must replace the singular velocity of a true point vortex by a smoothed velocity field. Mathematically, this means replacing the singular Biot–Savart kernel

$$\boldsymbol{K}(\boldsymbol{x}) = \frac{1}{2\pi|\boldsymbol{x}|^2}(-x_2, x_1) \tag{1.16}$$

by a smoothed or *mollified* kernel, such as the Gaussian kernel,

$$\boldsymbol{K}_\epsilon(\boldsymbol{x}) = \boldsymbol{K} \star \zeta_\epsilon = \frac{1}{2\pi|\boldsymbol{x}|^2}[1 - \exp(-|\boldsymbol{x}|^2\epsilon^{-2})](-x_2, x_1), \tag{1.17}$$

where $\star$ denotes convolution, ζ_ϵ is called the cut-off function and ϵ is a small parameter. Note that the mollified kernel (1.17) matches the singular kernel (1.16) when $|\boldsymbol{x}| \gg \epsilon$. Cottet & Koumoutsakos [7] show that the accuracy of the mollified kernel approximation increases with the number of vanishing moments of the cut-off function. The N vortex particles (defined by their positions $\boldsymbol{x}_p(t)$ and circulations $\Gamma_p(t)$) are then advected by the velocity field

$$\boldsymbol{u}(\boldsymbol{x}_p, t) = \boldsymbol{u}_\infty + \sum_{p=1}^{N} \boldsymbol{K}_\epsilon \star \Gamma_p \delta(\boldsymbol{x} - \boldsymbol{x}_p) \tag{1.18}$$

where $\boldsymbol{u}_\infty$ is the mean velocity, and $\delta(\boldsymbol{x})$ is the delta-function (i.e. the vortices are point particles). Note that because of the mollified kernel, the particles are not self-advected. At first glance the convolution calculation in equation (1.18) should increase the complexity of the method to $O(N^2)$, but grid-free methods exist (such as the fast multipole method [12]) that reduce the cost to $O(N \log N)$, or even $O(N)$. In practice, however, it is often more efficient to interpolate the vorticity onto a regular grid and use a fast Poisson solver to find the velocity. This makes the method semi-Lagrangian. Vortex methods have proved to be accurate and efficient for a wide range of vortical flows, especially wake flows in large domains [24].

It is appropriate at this point to compare the algebraic vortices of the numerical vortex method to stochastic and geometric vortices. The probabilistic representation of the vorticity equation shares many similarities with the numerical vortex method, especially when diffusion is introduced via white noise perturbations. There are, however, two fundamental differences. First, the vortex method consists of one realization made up of many thousands of particles, whereas the probabilistic representation consists of many realizations, each containing just one particle. Secondly, the vortex method smoothes the velocity field associated with the point vortices, whereas the probabilistic representation retains the singular velocity field. The probabilistic representation also explicitly includes the deformation tensor, which is absent in the vortex methods. It would be interesting to investigate further the links between vortex methods and probabilistic representations of the vorticity equation.

There are also links between the geometric and algebraic descriptions. In fact, the inviscid vortex method is based on the geometric idealization of point vortices, and some three-dimensional vortex methods use the slender vortex filaments discussed in section 1.2 as computational elements. Vor-

tex methods are also well-suited to exploring topological problems such as vortex reconnection [7]. On the other hand, the algebraic representation does not include any information about the coherence or incoherence of the vorticity being represented. The particles are the same whether they make up coherent vortices, or are part of the Gaussian noise. The algebraic vortices are, after all, simply computational elements.

1.4.2 *Adaptive wavelet method for the vorticity equation*

Finally, we consider an algebraic vortex method that combines some of the geometric and stochastic aspects discussed earlier. This is the WDNS method applied to the vorticity equation [41; 42]. (For WDNS applied to the Navier–Stokes equations in primitive form, please see [19].) We will see that WDNS may be classified as an Eulerian vortex method.

Grid adaptation occurs naturally in wavelet methods. Consider $\omega(\boldsymbol{x})$, defined on a closed two-dimensional rectangular domain Ω. We use tensor product second generation wavelets [39] constructed on a set of grids,

$$\mathcal{G}^j = \left\{ \boldsymbol{x}^j_{\boldsymbol{k}} \in \Omega : \boldsymbol{k} \in \mathcal{K}^j \right\}, \quad j \in \mathcal{J}, \tag{1.19}$$

where $\boldsymbol{k} = (k_1, \ldots, k_n)$ and grid points $\boldsymbol{x}^j_{\boldsymbol{k}} = (x^j_{1,k_1}, \ldots, x^j_{n,k_n})$ are constructed as a tensor product of uniformly spaced one-dimensional grids. The only restriction is that each individual set of one-dimensional grids is nested ($x^j_{m,k_l} = x^{j+1}_{m,2k_l}$, $m = 1, 2$), which guarantees the nestedness of the grids, *i.e.* $\mathcal{G}^j \subset \mathcal{G}^{j+1}$. The procedure for constructing two-dimensional scaling functions $\phi^j_{\boldsymbol{k}}(\boldsymbol{x})$ and a family of two-dimensional wavelets $\psi^{\mu,j}_{\boldsymbol{l}}(\boldsymbol{x})$, $\mu = 1, \ldots, 3$ on two-dimensional dyadic grid is described by Sweldens [39]. Once wavelets and scaling functions are constructed, the vorticity $\omega(\boldsymbol{x})$ can be decomposed as

$$\omega(\boldsymbol{x}) = \sum_{\boldsymbol{k} \in \mathcal{K}^0} c^0_{\boldsymbol{k}} \phi^0_{\boldsymbol{k}}(\boldsymbol{x}) + \sum_{j=0}^{+\infty} \sum_{\mu=1}^{3} \sum_{\boldsymbol{l} \in \mathcal{L}^{\mu,j}} d^{\mu,j}_{\boldsymbol{l}} \psi^{\mu,j}_{\boldsymbol{l}}(\boldsymbol{x}). \tag{1.20}$$

For functions like $\omega(\boldsymbol{x})$ which contain isolated small scales on a large-scale background, most wavelet coefficients are small. Thus, we retain a good approximation even after discarding a large number of wavelets with small coefficients. Intuitively, the wavelet coefficient $d^{\mu,j}_{\boldsymbol{l}}$ is small unless $\omega(\boldsymbol{x})$ has variation on the scale of j in the immediate vicinity of wavelet $\psi^{\mu,j}_{\boldsymbol{l}}(\boldsymbol{x})$. In fact, the error incurred by ignoring coefficients with magnitude lower than

ϵ is $O(\epsilon)$.

A vorticity-adapted grid can therefore be constructed by filtering the vorticity in wavelet space, and then performing the inverse transform using only the significant wavelets. This automatically interpolates the vorticity onto the set of significant grid points (note that there is a unique grid point associated with each wavelet coefficient, so neglecting wavelets is equivalent to removing grid points). A localized one-dimensional function, and its corresponding multiscale adapted grid are shown in figure 1.2. Recall that in section 1.3 we mentioned that wavelet filtering corresponds to a de-noising of the vorticity field, and that the significant wavelet modes correspond to the coherent vortices of the flow.

When solving the vorticity equations an additional criterion for grid adaptation must be added to take into account flow dynamics. The computational grid should consist of grid points associated with wavelets whose coefficients are significant and also those which could become significant during a time step. In other words, the computational grid should also include the nearest neighbouring points in position and scale. This corresponds to a CFL criterion of one, and provides full dealiasing for quadratic nonlinearities. The grid is adapted in this way at each time step, and the equations are integrated in time using a standard technique for ordinary differential equations.

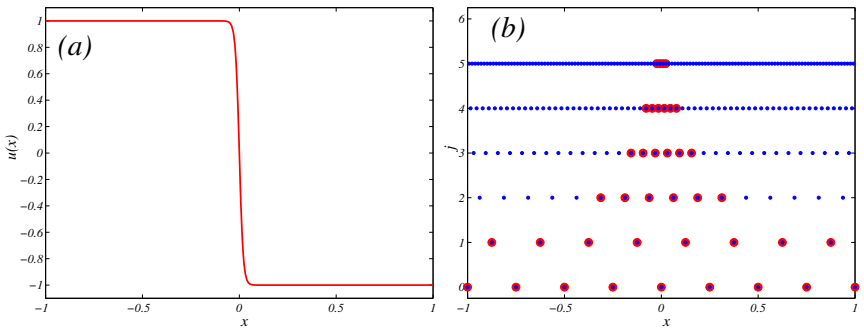

Fig. 1.2 Adaptive wavelet dyadic grid after Vasilyev & Bowman [41]. (a) Function. (b) Grid as a function of dyadic scale j and position x. Small points, uniform grid; large points, adapted grid. The actual computational grid is the union of the large points at all levels j.

When applied to the two-dimensional vorticity equations, WDNS constitutes an Eulerian vortex method. The adapted grid points may be thought

of as vortex particles with circulation given by their vorticity times the volume associated to the grid point. Indeed, we even use the fast multipole method [12] to calculate the velocity field from these vortex particles. Figure 1.3 shows the vorticity and adapted grid for periodic flow past a cylinder at $\mathrm{Re} = 20\,000$. Because the grid adapts to local gradients of vorticity, the distribution of points in the adapted grid resembles the distribution of point vortices in a vortex method. The main difference is that the grid points are densest where the gradients of vorticity are large, rather than where vorticity itself is large. (In fact, the WDNS grid for the Navier–Stokes equations [19] more closely resembles the locations of point vortices in the vortex method, since in this case the wavelets are sensitive to velocity gradients.) Although the vortex particles are restricted to a regular Cartesian grid, the fact that this grid can refine or coarsen as required to resolve the vorticity field means it is similar in spirit to a Lagrangian vortex method. One important distinction with respect to vortex methods is that in WDNS we resolve only the coherent vortices (if the threshold ϵ is set appropriately, as explained in section 1.3). Thus WDNS links algebraic, stochastic and geometric vortices.

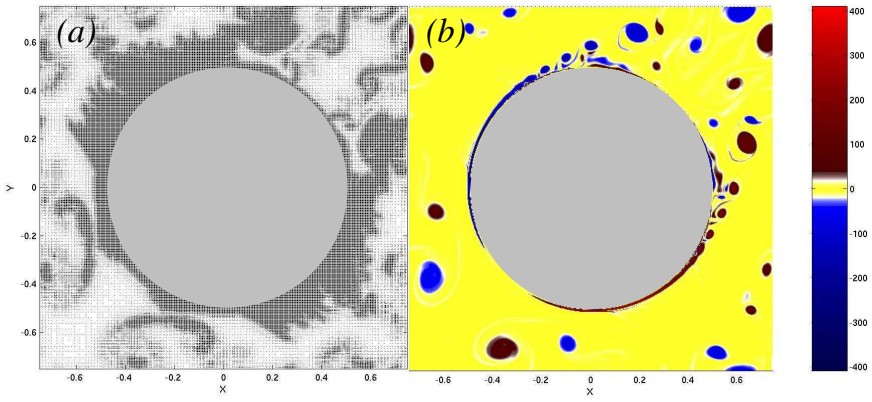

Fig. 1.3 WDNS simulation of flow past a periodic array of cylinders at $\mathrm{Re} = 20\,000$. (a) Adapted grid (including nearest neighbours in position and scale). (b) Vorticity.

1.5 Conclusions

This paper has looked at vortices from three different, but complementary, points of view: geometric, stochastic and algebraic. Vortices are not

only beautiful esthetically and mathematically elegant, they are also at the heart of many practical engineering applications. We began by showing how vortices are central to understanding such important problems in fluid dynamics as mixing, flow-induced vibration, turbulence and noise. We then saw how the geometric, stochastic and algebraic points of view each provide insight into the structure, dynamics and function of vortices. In particular, we saw how these different points of view help us to understand the role of vortices in complicated flows, such as turbulence. Finally, the wavelet direct numerical simulation (or coherent vortex simulation) showed how each of the three mathematical approaches can be combined in a single model.

Acknowledgment

Research funding from NSERC is gratefully acknowledged. This paper was written during a visit to DAMTP, University of Cambridge, and I would like to thank them for their hospitality.

Bibliography

1. Beale, J. and Majda, A. (1982). Vortex method I: Convergence in three dimensions. *Math. Comput.* **39**, 1–27.
2. Beale, J. and Majda, A. (1982). Vortex method II: High order accuracy in two and three dimensions. *Math. Comput.* **39**, 29–52.
3. Berkooz, G., Holmes, P. and Lumley, J. (1993). The proper orthobonal decomposition in the analysis of turbulent flows. *Annu. Rev. Fluid Mech.* **25**, 539–575.
4. Bonnet, J. P., Delville, J., Glauser, M. N. *et al.* (1998). Collaborative testing of eddy structure identification methods in free turbulent shear flows. *Experiments in Fluids* **25**, 197–225.
5. Busnello, B., Flandoli, F. and Romito, M. (2003). A probabilistic representation for the vorticity of a 3D viscous fluid and for general systems of parablic equations. In *Summer program: probability and partial differential equations in modern applied mathematics*. IMA.
6. Chorin, A. (1973). Numerical study of slightly viscous flow. *J. Fluid Mech.* **57**, 785–796.
7. Cottet, G. and Koumoutsakos, P. (2000). *Vortex methods: theory and practice*. Cambridge University Press.
8. Cottet, G.-H. and Poncet, P. (2002). Particle methods for direct numerical simulations of three-dimensional wake flows. *J. Turbulence* **3**, 1–9.
9. Donoho, D. L. (1993). Wavelet shrinkage and w.v.d. – a ten-minute tour. Technical Report 416, Dept. of Statistics, University of Stanford.
10. Farge, M., Schneider, K. and Kevlahan, N. K.-R. (1999). Non-gaussianity and coherent vortex simulation for two-dimensional turbulence using an adaptive orthogonal wavelet basis. *Phys. Fluids* **11**, 2187–2201.
11. Frisch, U. (1995). *Turbulence : the legacy of A.N. Kolmogorov*. Cambridge University Press.
12. Greengard, L. and Rokhlin, V. (1987). A fast algorithm for particle simulations. *J. Comput. Phys.* **73**, 325–348.
13. Griebel, M. and Koster, K. (2000). Adaptive wavelet solvers for the unsteady incompressible navier stokes equations. In J. Malek, J. Necas and M. Rokyta (editors), *Lecture Notes of the Sixth International School*

"Mathematical Theory in Fluid Mechanics", Advances in Mathematical Fluid Mechanics. Springer Verlag.

14. Griebel, M. and Koster, K. (2002). Multiscale methods for the simulation of turbulent flows. In E. Hirschel (editor), *DFG/CNRS Workshop, Nice, 2001, Notes on Numerical Fluid Mechanics*. Vieweg-Verlag.
15. Hunt, J., Wray, A. and Moin, P. (1988). Eddies, stream, and convergence zones in turbulent flows. Technical Report CTR-S88, Center for Turbulence Research.
16. Jeong, J. and Hussain, F. (1995). On the identification of a vortex. *J. Fluid Mech.* **285**, 69–94.
17. Jiménez, J. and Wray, A. (1998). On the characteristics of vortex filaments in isotropic turbulence. *J. Fluid Mech.* **373**, 255–285.
18. Kambe, T., Minota, T., Murakami, T. *et al.* (1990). Oblique collision of two vortex rings and its acoustic emission. In H. Moffatt and A. Tsinober (editors), *Topological fluid mechanics: proceedings of the IUTAM symposium, Cambridge, August 13–18, 1989*. 515–524.
19. Kevlahan, N. and Vasilyev, O. (2003). An adaptive wavelet collocation method for fluid–structure interaction at high reynolds numbers. *SIAM J. Sci. Comput.* To appear.
20. Kevlahan, N. K.-R. (1997). The vorticity jump across a shock in a non-uniform flow. *J. Fluid Mech.* **341**, 371–384.
21. Klein, R., Knio, O. and Ting, L. (1996). Representation of core dynamics in slender vortex filament simulations. *Phys. Fluids* **8**, 2415.
22. Klein, R. and Majda, A. (1991). Self-stretch of a perturbed vortex filament. *Physica D* **49**, 323.
23. Klein, R., Majda, A. J. and Damodaran, K. (1995). Simplified equations for the interactions of nearly parallel vortex filaments. *J. Fluid Mech.* **288**, 201–248.
24. Koumoutsakos, P. and Leonard, A. (1995). High-resolution simulations of the flow around an impulsively started cylinder using vortex methods. *J. Fluid Mech.* **296**, 1–38.
25. Krasny, R. (1986). A study of singularity formation in a vortex sheet by the point vortex approximation. *J. Fluid Mech.* **167**, 65–93.
26. Leonard, A. (1980). Vortex methods for flow simulation. *J. Comput. Phys.* **37**, 289–335.
27. Lesieur, M. and Métais, O. (1997). New trends in large-eddy simulations of turbulence. *Annu. Rev. Fluid Mech.* **28**, 45–82.
28. Lighthill, J. (2001). *Waves in fluids*. Cambridge University Press.
29. Lumley, J. (1967). The structure of inhomogeneous turbulent flow,. In A. Yaglom and V. Tatarski (editors), *Atmospheric Turbulence and Radio Wave Propagation*. Nauka, 160–178.
30. Majda, A. and Bertozzi, A. (2002). *Vorticity and incompressible turbulence*. Cambridge University Press.
31. Nazarenko, S., Kevlahan, N. K.-R. and Dubrulle, B. (2000). Nonlinear RDT theory of near-wall turbulence. *Physica D* **139**(158–176).
32. Noca, F., Shiels, D. and Jeon, D. (1997). Measuring instantaneous fluid dy-

namics forces on bodies, using only velocity fields and their derivatives. *J. Fluids Struct.* **11**, 345–350.
33. Noca, F., Shiels, D. and Jeon, D. (1999). A comparison of methods for evaluating time-dependent fluid dynamic forces on bodies, using only velocity fields and their derivatives. *J. Fluids Struct.* **13**, 551–578.
34. Prager, W. (1928). Die druckverteilung an körpern in ebener potentialströmung. *Phys. Z.* **29**, 865–869.
35. Provenzale, A. (1999). Transport by coherent barotropic vortices. *Annu. Rev. Fluid Mech.* **31**, 55–93.
36. Rosenhead, L. (1931). The formation of vortices from a service of discontinuity. *Proc. R. Soc. London Ser. A* **134**, 170–192.
37. Saffman, P. (1992). *Vortex dynamics*. Cambridge University Press.
38. Schneider, K., Kevlahan, N. K.-R. and Farge, M. (1997). Comparison of an adaptive wavelet method and nonlinearly filtered pseudo-spectral methods for two-dimensional turbulence. *Theoret. Comput. Fluid Dynamics* **9**, 191–206.
39. Sweldens, W. (1996). The lifting scheme: A custom-design construction of biorthogonal wavelets. *Appl. Comput. Harmon. Anal.* **3**(2), 186–200.
40. Ting, L. and Klein, R. (1991). *Viscous vortical flows*. Springer.
41. Vasilyev, O. V. and Bowman, C. (2000). Second generation wavelet collocation method for the solution of partial differential equations. *J. Comput. Phys.* **165**, 660–693.
42. Vasilyev, O. V. and Kevlahan, N. K.-R. (2002). Hybrid wavelet collocation-brinkman penalization method for complex geometry flows. *Int. J. Num. Meth. Fluids* **30**, 531–538.
43. Yokokawa, M., Itakura, K., Uno, A. *et al.* (2002). 16.4-Tflops direct numerical simulation of turbulence by a fourier spectral method on the earth simulator. In *Proceedings of the Proceedings of the IEEE/ACM SC2002 Conference*. IEEE Computer Society, 50.
44. Zhou, H. (1997). On the motion of slender vortex filaments. *Phys. Fluids* **9**, 970–981.